

# From Boiling Stones to Smart Crystals: Supramolecular and Magnetic Isotope Control of Radical–Radical Reactions in Zeolites

NICHOLAS J. TURRO

Department of Chemistry, Columbia University, 3000 Broadway, MC 3119, New York, New York 10027

Received March 6, 2000

## ABSTRACT

The chemistry of radicals adsorbed on zeolites is remarkable in that the products of radical–radical reactions, which are nonselective in solution, can be made selective and can be controlled by supramolecular effects and magnetic isotope effects. The photolysis of ketones adsorbed on zeolites can be manipulated so that either primary or secondary radicals produced by photolysis can be directed to selected radical–radical reactions which are unknown in solution.

## Introduction

Zeolites are inorganic solids that are close relatives to the soil, sand, minerals, and clays that make up much of the earth around us.<sup>1–4</sup> According to zeolite lore,<sup>5</sup> in 1756 a Swedish mineralogist, Baron Axel F. Cronstedt, discovered that certain crystalline minerals found near volcanic deposits appear to “boil” when heated. These crystals survived repeated heating–boiling–cooling cycles. Cronstedt named these crystals “zeolites” from two Greek roots, *zeo*, “to boil”, and *lithos*, “stone”. The boiling phenomenon is the result of reversible adsorption/expulsion of water from the porous internal void space and internal surface of zeolite crystals.

Zeolites are widely employed in the catalytic and separation sciences. Important technological applications<sup>1–4</sup> include the manufacture of gasoline from methanol, the catalytic cracking of crude oils into high-quality fuels, and the separation of *p*-xylene from *o*-xylene and *m*-xylene. The improvement in petroleum cracking efficiency provided by zeolites permits the saving of billions of dollars a year.<sup>4</sup> Zeolite catalysis is controlled by the same porous internal structure of zeolites that is responsible for the reversible adsorption of water. The humble “boiling stones” of Cronstedt might today be elevated to the status of “smart crystals”, capable of remarkable catalysis and separations resulting from *molecular recognition*. The

“Philosopher’s Stone” was the Alchemist’s visionary catalyst to transform plentiful and base metals such as lead into valuable metals such as gold. Indeed, a zeolite, as a smart crystal, may be considered a modern day Philosopher’s Stone, which can transform plentiful and base materials such as crude oil into valuable materials such as high-grade fuels.

Several reviews of the photochemistry of organic molecules adsorbed on zeolites have appeared.<sup>6–9</sup> In this Account, we describe the application of supramolecular concepts involving the size/shape structural aspects of the void space of zeolites, to control the selectivity of reactions of radicals produced by photochemical excitation of organic molecules adsorbed on zeolites. In particular, we examine the photochemical reactions of ketones which generate reactive carbon-centered radicals that are structurally similar to those involved in zeolites’ catalytic applications. However, the strongly acidic active sites that are important in catalytic applications have been removed by exchange with alkali ions. This allows size/shape parameters, along with surface sieving and diffusional parameters, to be examined in the absence of effects due to the chemical activation by zeolites by acidic sites. Activation is provided by photoexcitation of ketones adsorbed on zeolites at room temperature and produces well-defined radical species whose reactivity is controlled by *supramolecular features* of adsorbed radicals. A “geminate” (born together) radical pair is produced by photolysis of a specific supramolecular structure, and the chemical fate of radical fragments is determined by the rotational and diffusional pathways and size and shape of the space accessible to the radicals between the time the primary geminate pair is created and the time in which irreversible radical–radical reactions occur.

## The MFI and FAU Families of Zeolites

Zeolites<sup>1–4</sup> are crystalline aluminosilicates constituted by oxygen (corner) sharing tetrahedral  $\text{AlO}_4$  and  $\text{SiO}_4$  groups that form a *rigid* three-dimensional network termed the *zeolite framework*. Each of the  $\text{AlO}_4$  tetrahedra possesses a formal negative charge, which requires charge compensation by cations. “Classical” zeolites possess the composition  $\text{M}_x(\text{AlO}_2)_x(\text{SiO}_2)_y$ , where M may be, for example, a monovalent cation ( $\text{H}^+$ ,  $\text{Li}^+$ ,  $\text{Na}^+$ ,  $\text{K}^+$ ) required for charge compensation. The carbon radicals produced by photoexcitation are inert toward reaction with the zeolite framework and cations. This feature allows us to concentrate on supramolecular features of *radical–radical reactions*, which determine the observed products and radical persistence.

Silicalite<sup>10</sup> and ZSM-5<sup>11</sup> are important members of the “MFI” family of zeolites, whose internal surface or “void space” consists of channels and intersections (“super-cages”) formed by the framework walls (Figure 1). The channels are cylindrical (diameters ca. 5.5 Å), and the

Nicholas J. Turro has been teaching at Columbia University since 1964 and is currently the Wm. P. Schweitzer Professor of Chemistry and co-chair of the Department of Chemical Engineering and Applied Chemistry, as well as Professor of Earth and Environmental Engineering. He has written over 650 scientific publications and two textbooks on molecular photochemistry. Recent awards include the 1999 ACS Award in Colloid or Surface Chemistry and the Willard Gibbs Medal of the Chicago Section of the ACS. He is a member of the National Academy of Sciences and the American Academy of Arts and Sciences.

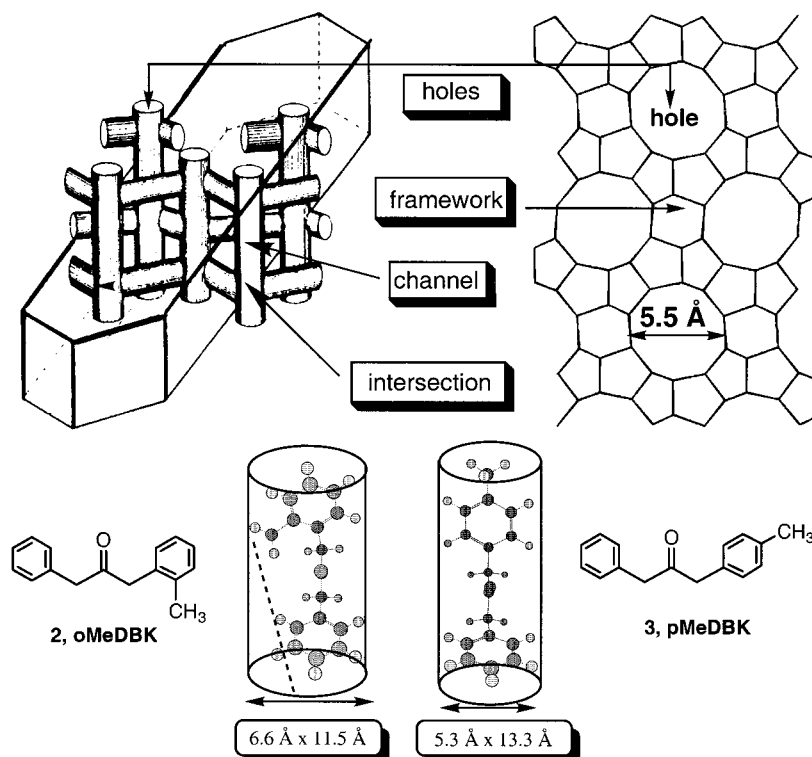


**FIGURE 1.** Schematic representation of the structure of the MFI family of zeolites. The vertices represent Si atoms or Al atoms bound by oxygen atom bridges, which are represented by the lines between vertices. The internal void space structure is shown on the left in relation to a crystal. The external surface is shown on the right. The minimal cylindrical cross sections of two of the ketones discussed in the Account are shown at the bottom of the figure. The ortho isomer, **2**, does not have access to the internal surface because its minimum cross section is larger than the holes on the external surface. The para isomer, **3**, is allowed access to the internal surface.

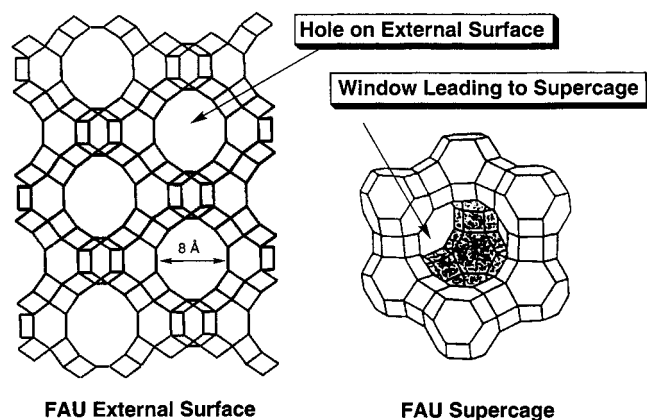


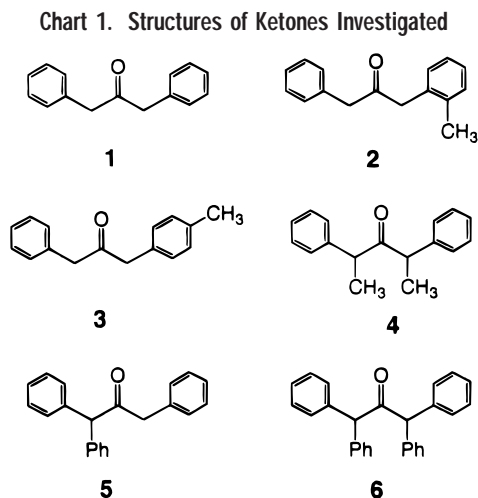
**FIGURE 2.** Schematic representation of the structure of the FAU family of zeolites. As in Figure 1, the vertices represent Si atoms or Al atoms bound by oxygen atom bridged, which are represented by the lines between vertices. The external surface is shown on the left, and a supercage, which is the main structural void space unit of the internal surface, is shown on the right. All of the ketones employed in this investigation have access to the supercages of the FAU zeolites.

intersections are spherical (diameter ca. 9 Å). The external surface of an MFI zeolite crystal consists of the framework and pore openings (“holes”). The holes on the external surface provide access to the internal surface, but only to molecules whose size/shape characteristics allow penetration into the holes and whose mobility allows diffusion into the internal surface.

The “FAU” zeolites (Figure 2), of which the “X” and “Y” zeolites are important members, constitute a second important zeolitic family. The X zeolite possesses more (negatively charged) Al atoms in its framework and therefore possesses more compensating cations in its internal surface. The internal surface of both X and Y zeolites consists of spherical supercages approximately 13 Å in diameter. Access to the supercages is provided by “windows” (ca. 8 Å diameters) on the external surface. The supercages form a three-dimensional network of void space in which each supercage is tetrahedrally connected to four other supercages. The MFI and FAU families of zeolites provide different void spaces for the photochemistry of ketones to be examined in this Account.

## Zeolites as Enzyme Mimics

The outstanding size/shape selectivity of zeolites as catalysts is reminiscent of the guest/host selectivity of enzymatic reactions.<sup>12,13</sup> Zeolites possess a number of structural properties analogous to the protein coat and active site of natural enzymes. The active site of an enzyme operates similarly to a *microscopic reaction vessel*<sup>14</sup> which confines and directs the chemistry of the bound substrate. The enzyme’s protein tertiary structure captures substrates by adsorption on its external surface, and then the sieving of substrate molecules is directed so that only those molecules capable of diffusing through the “protein



channels” can achieve access to the internal active sites. The active site possesses size and shape characteristics which determine the selectivity of substrate reactions. In the analogy with zeolites, the protein mantle is replaced by the zeolite framework and the active sites are replaced by the holes on the external surface and the supercages of the internal surface (Figures 1 and 2) of the zeolite.

### Adsorption of Dibenzyl Ketones on Zeolites. Supramolecular Considerations

Chart 1 shows the structures of the ketones, **1–6**, investigated in this Account. From Figure 1 we can deduce that, for the ketone@MFI systems (the @ indicates adsorption of a guest ketone to a host zeolite), only **1** and **3** (minimum molecular cross sections  $<5.5$  Å) will fit into the holes (ca.  $5.5$  Å) on the external surface and have access to the internal surface of the MFI zeolites. On the other hand, **2**, **4**, **5**, and **6** (minimum molecular cross sections  $>5.5$  Å) will be able to intercalate a benzene ring into a hole on the external surface but will not be able to enter the internal surface of MFI zeolites. **1** and **3**, once adsorbed into the internal surface of an MFI zeolite, should be adsorbed at the relatively spacious intersections. On the other hand (Figure 2), for the ketone@FAU systems, all of the ketones, **1–6**, possess minimum molecular cross sections smaller than the  $8$  Å windows of the external surface and can readily enter the supercages of the internal surface.

### Photochemical Production of Geminate Radical Pairs. Radical–Radical Reaction Pathways

A general and simplified paradigm<sup>15</sup> for the photochemistry of all of the ketones, **1–6**, is given in Figure 3 (ketones represented as ACOB). Photochemical excitation in each case causes  $\alpha$ -cleavage to produce a *primary, geminate radical pair*, which may undergo radical–radical combination reactions (path 1) in competition with decarbonylation (path 2) to produce a *secondary, geminate radical pair*. The latter may undergo radical–radical secondary geminate combination (path 3) in competition with formation of *free radicals* (path 4). The free radicals

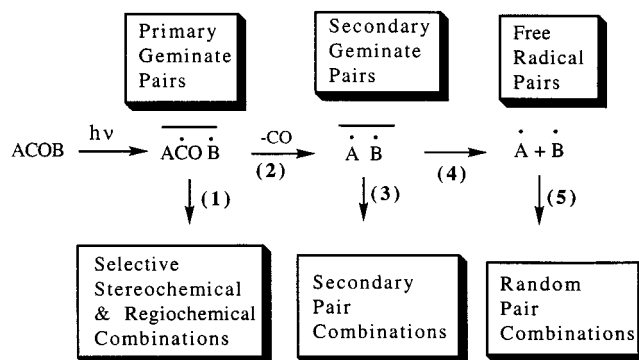


FIGURE 3. Paradigm for the photolysis of dibenzyl ketone and related ketones. See text for discussion.

undergo random radical–radical combination reactions (path 5). In solution, photolysis of **1–6** results in nonselective free radical combination reactions.<sup>8</sup> We shall show how photolysis of **1–6**@zeolites allows (1) selective stereochemical and regiochemical combination of the geminate primary pairs; (2) selective combination reactions of geminate secondary pairs; and (3) selective combination reactions of random radical pairs.

### Reactions of Radicals Adsorbed on Zeolites. Supramolecular Control of Radical–Radical Reaction Pathways

Ordinary catalysts accelerate reaction rates through interaction of a substrate and the catalyst, which causes certain critical bonds to be weakened through supramolecular interactions. In reactions considered in this Account, critical bonds are not weakened by interaction with the zeolite but are broken by the absorption of light, which causes the formation of reactive intermediates (radicals) without any activation from the zeolite. Thus, in contrast to conventional catalysis, the bond-breaking process does not depend on the site of adsorption of the substrate: the “active site” for radical pair formation is simply where the substrate happens to be when it absorbs a photon.

The basic strategy behind the supramolecular control of radical–radical reactions is to use the *supramolecular structure and dynamics* of the initially formed primary pair and subsequent radical species to determine the chemical options (Figure 3). This strategy is implemented through control of (1) the *initial* supramolecular structure of the ketone@zeolite complex together with (2) the *accessible pathways of diffusion and rotation* available to the primary and secondary radicals. With this strategy, we shall show that the photochemistry of **1–6**@zeolite can be rationally, systematically, and selectively directed to one of the product pathways shown in Figure 3.

### Photochemistry of Ketones Adsorbed on MFI Zeolites. Supramolecular Effects on Radical–Radical Reactions of Secondary Radicals

An important industrial application of MFI zeolites involves the separation of *p*-xylene from *o*-xylene and

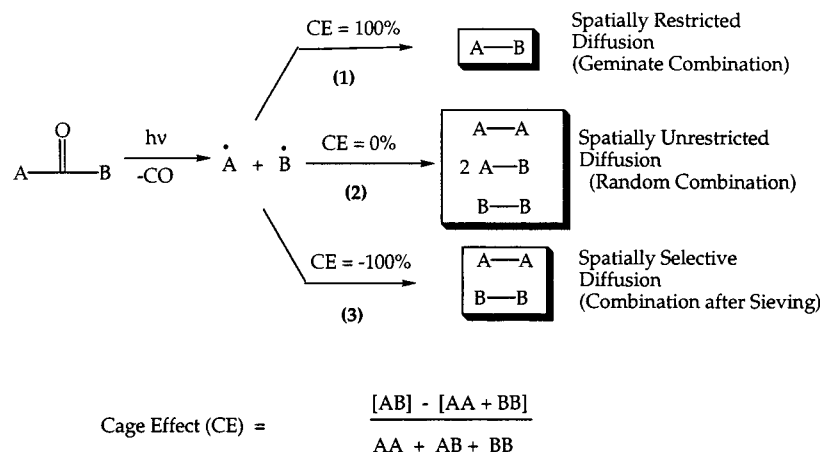


**FIGURE 4.** Three limiting “cage effects” for secondary radical–radical combinations. The cage effect is defined in terms of the product ratios observed in the photolysis as shown in the figure.

*m*-xylene.<sup>2–4</sup> The minimum molecular cross section of *p*-xylene is ca. 5.5 Å, approximately the size of the holes on the external surface of an MFI crystal (Figure 1), whereas both *m*-xylene and *o*-xylene possess molecular cross sections that are greater than 5.5 Å. Whereas *o*-xylene and *m*-xylene must reside on the external surface, *p*-xylene is readily adsorbed into the internal surface of MFI zeolites. Thus, **2** (minimum molecular cross section similar to *o*-xylene) and **3** (minimum molecular cross section similar to *p*-xylene) are expected to exhibit distinct and different supramolecular structures and distinct supramolecular photochemistry when adsorbed on MFI zeolites.

Photolysis of **2** or **3** adsorbed on “dry” MFI zeolites (samples in which the solvent employed to deposit the ketone on the zeolite is removed by evaporation before photolysis) produces only radical–radical combinations of secondary radicals. Thus, the decarbonylation of primary pairs (Figure 3, path 2) occurs much faster than the recombination of primary pairs (Figure 3, path 1). It has been useful to analyze product distributions in terms of three possible pathways<sup>18</sup> for radical–radical reactions from the secondary radicals produced from the photolysis of **2** or **3** (represented as ACOB, where A is the methyl-substituted ring in Figure 4). These pathways may be expressed quantitatively in terms of “cage” effects. If the only combination product is AB, this corresponds to 100% secondary *geminate* pair combination (termed a positive cage effect). If the only products are AA and BB, this corresponds to 100% *sieving* separation of the geminate pairs followed by combination of the separated partners (termed a negative cage effect). If the products are AA, AB, and BB (in the ratio of 25:50:25), this corresponds to *random* coupling of the radicals after free radical formation (termed a zero cage effect).

In nonviscous solutions, photolysis of ketones such as **2** or **3** gives cage effects close to zero.<sup>19</sup> This means that in solution the “walls” of the solvent cannot constrain the geminate pair effectively so that free radicals are formed efficiently.

### Photolysis on the Internal Surface. Geminate Combination

Photolysis<sup>18</sup> of **3** (pACOB@MFI) leads to pAB (Figure 4, path 1) as the dominant product. Photolysis produces a primary geminate pACO/B radical pair constrained in a space of ca. 9 Å. This is enough space for the pair to separate a few angstroms for a time sufficient for decarbonylation (which takes ca. 100 ns in solution<sup>20,21</sup>) and to produce a secondary *geminate* radical pair, pA/B. The latter pair is constrained by the “walls” of the framework of the intersection, which serves as a “supercage” for the two radicals and which inhibits diffusional separation and allows secondary geminate combination (positive cage effect) to occur efficiently (Figure 5A). This result demonstrates how the zeolite “supercages” provide for a certain degree of separation (allowing time for efficient decarbonylation), but which still encourage geminate recombination of the secondary pair.

### Photolysis on the External Surface. Sieving and Random Combinations

Photolysis<sup>18</sup> of **2** (oACOB@MFI) results in formation of oAoA + BB as major products at low coverages (negative cage effect, Figure 4, path 3) and to 25% oAoA + 50% oAB + 25% BB at higher coverages (zero cage effect, Figure 4, path 2). The surface coverage dependence of the photochemistry of oACOB@MFI is consistent with a two-site model for adsorption on the external surface (Figure 5) in which *the holes are filled first and then the external framework is filled until a monolayer is formed*.

Since the number of “moles of holes” on the external surface is finite, the photochemistry of oACOB will change after the holes are filled. At low coverages (Figure 5 B, left), the benzene (B) ring of oACOB intercalates into a hole on the external surface to produce a supramolecular structure oA<sub>ex</sub>COB<sub>in</sub>@MFI. Photolysis of oA<sub>ex</sub>COB<sub>in</sub>@MFI produces, after rapid decarbonylation, a secondary radical pair consisting of a B<sub>in</sub> bound to a hole and an oA<sub>ex</sub> radical that is free to diffuse on the external surface. The products



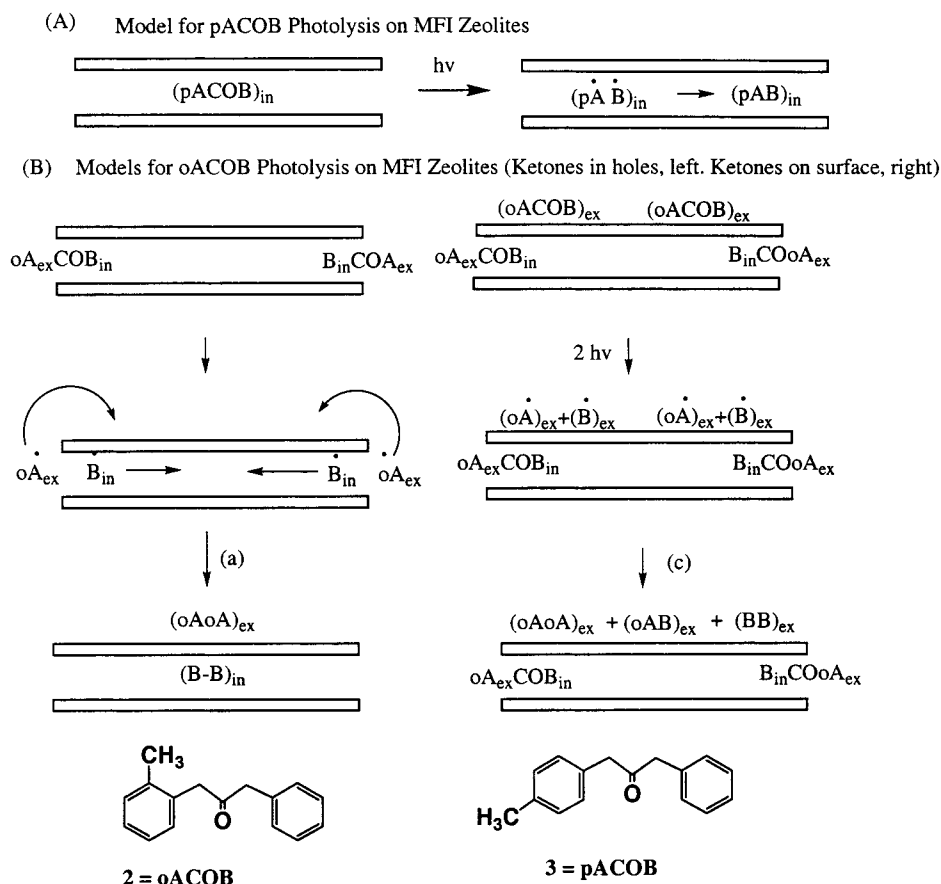


FIGURE 5. Schematic representation of the cage effects. (A) Photolysis of 3@MFI. (B) Left: Photolysis of 2@MFI in the holes (a low coverage situation). Right: Photolysis of 2@MFI on the external framework (a high conversion situation).

are determined by the diffusional pathways available to the *two spatially distinct radicals*,  $oA_{ex}$  and  $B_{in}$ . The  $B_{in}$  in the hole is well positioned to diffuse into the internal surface, where it will only encounter  $B_{in}$  radicals from other photolyses but will not encounter  $oA_{ex}$  radicals, which are denied access to the internal surface. When two  $B_{in}$  radicals encounter at an intersection of the internal surface, there is sufficient space for  $B_{in} + B_{in}$  radical–radical combination to produce  $(BB)_{in}$ . However, the  $oA_{ex}$  radicals diffuse on the external surface, where they encounter other  $oA_{ex}$  radicals to produce  $(oAoA)_{ex}$ . Thus, when only the holes are occupied (Figure 5B, left),  $(oAoA)_{ex} + (BB)_{in}$  are the major products of photolysis.

After all the holes are filled (Figure 5B, right), a second *isomeric* supramolecular structure,  $(oACOB)_{ex}$ , is formed. Radicals produced by photolysis of  $(oACOB)_{ex}$  are able to diffuse randomly on the external surface. However, because all of the holes are filled first, neither radical can be sieved into the internal surface. As the fraction of framework-bound ketones increases, an increasingly greater fraction of free radicals will be produced from photolysis of  $(oACOB)_{ex}$ . Therefore, a negative cage effect is observed for low loadings (Figure 4, path 3), and the cage effect tends toward zero (Figure 4, path 2) as the loading is increased. This model is consistent with the results of solid-state NMR analysis.<sup>22,23</sup>

## Supramolecular Steric Effects on Radical–Radical Reactions

Gomberg's report<sup>24</sup> of the preparation of the triphenylmethyl radical (TPM) launched the field of "persistent carbon centered" free radicals, i.e., radicals able to survive at room temperature. The persistence of carbon-centered radicals often depends on *molecular steric factors* that hinder radical–radical combination reactions.<sup>17</sup> The rate of radical–radical reactions determines the persistence of all radical@zeolite species discussed in this Account. The ability of a radical to react with a second radical in a zeolite intersection will depend on the space available for radical–radical reaction (combination or disproportionation) in the intersection. Thus, "supramolecular" steric effects may hinder or completely suppress certain radical–radical reactions selectively, *even those occurring at close to diffusional rates in solution*. Related behavior in enzymes has been termed<sup>25</sup> "negative catalysis", in which certain pathways are favored not by acceleration but by hindrance of fast pathways that are favored in solution.

## Supramolecular Steric Effects on Chemoselectivity of Radical–Radical Reactions

Supramolecular steric effects on the chemoselectivity radical–radical reactions are revealed by comparison of

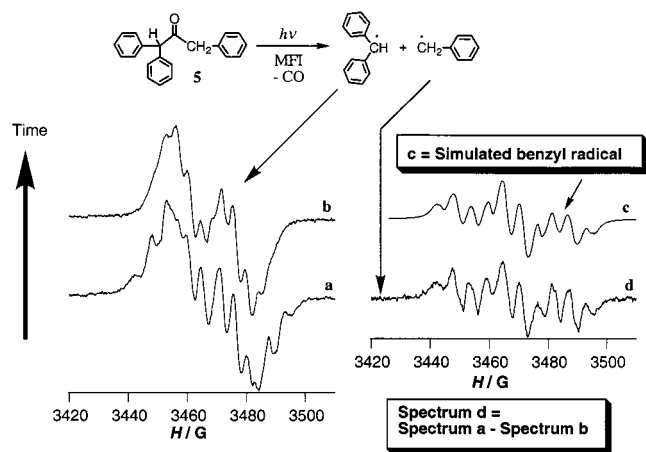
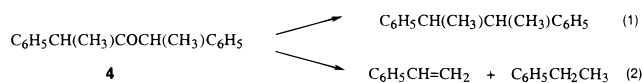


**FIGURE 6.** EPR spectra (a–c) of a photolyzed sample of **5**@MFI. Spectra a and b were produced under degassed conditions 5 min and 5 h after irradiation of the sample. Spectrum c was obtained by subtracting b from a.

the photochemistry of **1**<sup>18</sup> and **4**<sup>23</sup> adsorbed on MFI zeolites. For the **1**@MFI combination product, 1,2-diphenylethane (95%) dominates; for **4**@MFI, however, disproportionation products styrene and ethylbenzene (75%) are formed (eqs 1 and 2). Benzyl ( $C_6H_5CH_2$ ) radicals from



photolysis of **1**@MFI undergo radical–radical combination in the intersections. However, for methylbenzyl ( $C_6H_5CHCH_3$ ) radicals from photolysis of **4**@MFI, the intersections impose severe steric hindrance toward radical–radical combination to form 2,3-diphenylbutane, the dominant product formed (95%) in fluid solution (eq 1). Two  $C_6H_5CHCH_3$  radicals form the disproportionation products (eq 2), because transfer of a hydrogen atom from one radical to the other is less sterically demanding than combination. Thus, the major products of the “molecular” photochemistry of **4** in solution and the supramolecular photochemistry of **4**@MFI differ dramatically because of the supramolecular steric effects which selectively favor radical–radical disproportionation over combination in the intersections.

### Supramolecular Steric Effects on Radical Persistence

Examples of supramolecular steric effects causing radical persistence are available from EPR and fluorescence analysis<sup>23,26–29</sup> of the photolysis of **4**–**6**@MFI. The photolysis of each of these ketones produces readily observable EPR (Figure 6) and fluorescence signals. In the case of **5**@MFI, the EPR spectrum changes with time (a → b in Figure 6) and then remains constant. The final spectrum (Figure 6b) is assigned to the diphenylmethyl radical. The same spectrum<sup>27</sup> is produced by photolysis of **6**@MFI. Subtraction of the final spectrum (b) from the initial spectrum (a) generates a spectrum (d) which is assigned

**Table 1. Product Distributions (%) for the Photolysis of **1**@MX and **1**@MY Zeolites**

zeolite	DPE	oMAP	pMAP
LiX	81	3	16
NaX	55	17	26
KX	40	40	16
LiY	100	0	0
NaY	95	0	5
KY	94	2	4

to the benzyl radical by simulation (Figure 6c). The benzyl radical persists with a half-life of about an hour, whereas the diphenylmethyl radical (DPM) is persistent for days!

The  $C_6H_5CHCH_3$  radical derived from photolysis of **4**@MFI possess a half-life of the order of several hours, longer than those of adsorbed benzyl radicals but shorter than those of diphenylmethyl radicals. Thus, in terms of *supramolecular reactivity*, the benzyl radicals undergo combination reaction in the intersections, the  $C_6H_5CHCH_3$  radicals undergo disproportionation in the intersections, and the diphenylmethyl radicals are incapable of undergoing any reaction in the intersections. In contrast, in nonviscous solvents, the *molecular reactivity* of all of these radicals<sup>17</sup> toward radical–radical combination is close to diffusion controlled, and none of the radicals is persistent. The addition of air to a sample of DPM causes a peroxy radical spectrum to appear.<sup>26,27</sup> Remarkably, when the sample is vacuum degassed, the EPR signal of the diphenylmethyl radical reappears, showing that the addition of molecular oxygen is reversible.<sup>26,30</sup>

### Photochemistry of Ketones Adsorbed on FAU Zeolites

The photochemistry of ketones<sup>8,26,27,31–34</sup> **1**–**6**@MFI involves radical–radical reactions of secondary radicals (both geminate and random). We now consider photochemistry in FAU zeolites, in which radical–radical reactions of primary geminate pairs can be made to occur selectively. The void space of the FAU zeolites differs from that of MFI zeolites (compare Figures 1 and 2) in that the holes on the external surface of the FAU zeolites (ca. 8 Å) are significantly larger than the holes on the external surface of the MFI zeolites (ca. 5.5 Å). The internal structure of FAU zeolites consists of supercages (ca. 13 Å) that are larger than the intersections (ca. 9 Å) of the MFI zeolites. Importantly, the FAU internal surface contains a large concentration of compensating cations in the supercages.

We shall consider two FAU zeolites, “MX” and “MY”, where M refers to the compensating cation. Both zeolites possess the same supercage structure, but the “X” zeolite possesses a higher concentration of cations than the “Y” zeolite. A supercage of either FAU zeolite may easily accommodate any one of the ketones (**1**–**6**), in addition to a certain number of cations and even a co-guest organic molecule.

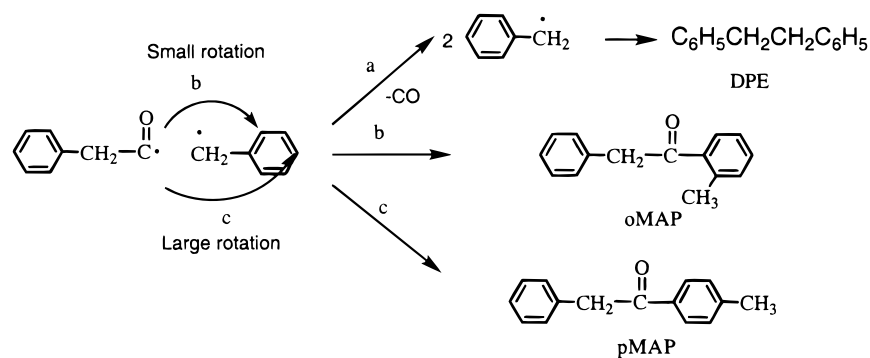


**FIGURE 7.** Model for the reaction of the primary radical pair produced by photolysis of **1@FAU**. Option a is separation and decarbonylation followed by combination to form DPE. Options b and c involve recombinations of the primary pair to form regioisomers. pMAP is *p*-methyl- $\beta$ -phenylacetophenone and oMAP is *o*-methyl- $\beta$ -phenylacetophenone. See text for discussion.

### Supramolecular Control of Regioselectivity in Primary Radical Pair Combination Reactions. Cation Effects

Three products, DPE, oMAP, and pMAP (see Figure 7 for structures), are formed when **1@FAU** systems are photolyzed<sup>8,31,32</sup> such that each FAU supercage contains ca. one **1** molecule. The photochemistry of **1@MY** zeolites (Table 1) yields mainly 1,2-diphenylethane (DPE), *independent* of the cation (Li, Na, K).

In going from LiX to NaX to KX, there is a dramatic change in the products formed from radical–radical combinations (Table 1). The two regioisomers, pMAP and oMAP, result from *primary geminate radical pair recombination*. For LiX the major product is DPE (81%), but for KX the regioisomers are the major products (56%).

The space available for radical–radical reactions depends on the number and size of the cations occupying the supercage. The larger number of cations in the MX zeolite creates steric hindrance to radical–radical reactions occurring in the supercage and favors formation of regioisomers.

For the MY zeolites (lower concentration of cations), the steric effects on the primary pair in a supercage are smaller. Diffusional separation and decarbonylation to form secondary radicals occur and the secondary radicals combine to form DPE in a geminate or random fashion (Figure 7a). For the MX zeolites, steric effects due to cations become significant. For LiX (Table 1), the onset of steric effects is already apparent as a significant amount (ca. 20%) of primary pair recombination occurs to form regioisomers oMAP and pMAP. As the steric constraints due to cation density or size increase, *the amount of diffusional and rotational motion available to the primary geminate radical pair decreases and the fraction of primary recombination is expected to increase*. Indeed, for photolysis of **1@NaX**, the formation of significant yields of regioisomers (ca. 45%) indicates that diffusional separation and rotation followed by recombination are becoming competitive. For photolysis of **1@KX**, the regioisomers are the major products (ca. 60%). Furthermore, as steric effects increase, the formation of the least motion product from recombination, oMAP, becomes more favored rela-

tive to pMAP. Thus, the yields of DPE relative to regioisomers and the ratio of oMAP to pMAP are parameters that characterize control of diffusional and rotational motion due to steric constraints: (1) the larger the relative yield of DPE to the regioisomers oMAP and pMAP, the faster the diffusional separation of the partners of the primary pair relative to combination reactions of the primary pair (Figure 7a versus 7b + 7c); (2) the larger the relative yield of pMAP to oMAP, the faster the rotational separation of the partners of the primary pair (Figure 7c versus 7b). These results show how supramolecular structure can be manipulated to selectively favor primary pair reactions over secondary pair reactions and to selectively favor one regioisomer over another.

### Supramolecular Control of Regioselectivity in Primary Radical Pair Combination Reactions. Co-Guest Effects

Electrostatic effects of the cations in zeolites are expected to play a role in influencing product formation and are known to do so in other systems.<sup>35</sup> However, the role of electrostatics for the **1@FAU** systems appears to be minor. For example,<sup>36</sup> addition of benzene to LiX causes the product distribution to become similar to that found for NaX (Table 1), and the addition of benzene to NaX causes the product distribution to become similar to that found for KX. Addition of benzene to the MY zeolites causes a significant increase in the yield of regioisomers. Thus, the addition of nonpolar organic molecules as co-guests increases the steric constraints in the supercage in a manner analogous to increasing the cation size, so that the effects of either cation or co-guest are probably steric rather than electrostatic for the cases studied.

### Magnetic Isotope Effects on the Regioselectivity of Primary Geminate Radical Pair Recombination Reactions

An important structural feature not shown explicitly in Figure 3 is the fact that the initial primary geminate radical pair (ACO/B) is produced in a triplet state.<sup>15,37</sup> Triplet states are *inert to radical–radical combination and dis-*

*proportionation reactions*, since the products of these reactions are singlet molecules. Intersystem crossing from a triplet to a singlet state is required for radical–radical reactions of a triplet pair of radicals to occur. The time delay required for intersystem crossing allows physical processes such as relative rotation and diffusion of the pair or chemical processes such as decarbonylation and conversion of the pair to secondary radical pairs to compete with recombination of the primary geminate pair. By controlling the time of intersystem crossing and the lifetime of the pair, it is possible to control the extent of and the selectivity of primary geminate pair combinations.

Triplet radical pairs, generated by photolysis in supramolecular hosts that serve as “supercages”, are often subject to significant magnetic field and magnetic isotope effects.<sup>38</sup> The basis of these effects is the interplay of a distance-dependent electron exchange, hyperfine interactions, and the requirement for recombination reactions to be preceded by intersystem crossing (ISC) to a singlet pair. The rate of ISC of geminate radical pairs in supramolecular systems is often controlled by hyperfine coupling. If this is the case for triplet geminate radical pairs adsorbed in zeolites, *magnetic isotope effects* on the product yields of radical pairs are possible.

An example of magnetic isotope effect was found<sup>39</sup> for photolysis of two isotopomers, **1**-<sup>12</sup>CO@NaX (1% natural abundance <sup>13</sup>C) and **1**-<sup>13</sup>CO@NaX (90% enriched in <sup>13</sup>C at the carbonyl carbon). The photolysis<sup>16</sup> of **1**-<sup>12</sup>CO@NaX produces DPE (56%) as the major product, along with the regioisomers oMAP (17%) and pMAP (26%). However, the photolysis of **1**-<sup>13</sup>CO@NaX produces the regioisomers *o*-MAP (37%) and *p*-MAP (36%) as the major products. Thus, *the occurrence of a <sup>13</sup>C isotope at the carbonyl position of the primary pair increases ISC*, enhancing primary pair recombination to form regioisomers. This is because the <sup>13</sup>C isotope, being a magnetic nucleus, can accelerate ISC in the geminate triplet pair through hyperfine coupling, whereas the <sup>12</sup>C isotope, being nonmagnetic, cannot influence the rate of ISC. Faster formation of the singlet allows primary pair reactions to compete more favorably with diffusional and rotational motions of the pair. Thus, less DPE (diffusional separation product) and more regioisomers are produced when **1**-<sup>13</sup>CO@NaX is photolyzed relative to **1**-<sup>12</sup>CO@NaX. Impressively, for the regioisomers, the relative amount of *o*-MAP (least rotational motion product) is significantly higher for **1**-<sup>13</sup>CO@NaX than for **1**-<sup>12</sup>CO@NaX.

### Supramolecular Control of Stereochemistry in Primary Geminate Radical Pair Reactions. Enantiomeric Selectivity in Radical Pair Recombination Reactions

Enzymatic stereochemical selectivity is achieved by the binding of a substrate to a stereochemically demanding void space at the active site. Stereospecificity in “molecular” radical–radical combination reactions in fluid solutions is very difficult because of the rapid irreversible

**Table 2. Photolysis of *meso*-4 Adsorbed in NaY with Coloaded Ephedrine as Chiral Inductor**

ketone	chiral inductor	ee of d,l-1 (%)
<i>meso</i> -4- <sup>12</sup> CO	(–)-ephedrine	+4.7
<i>meso</i> -4- <sup>13</sup> CO	(–)-ephedrine	+9.0
<i>meso</i> -4- <sup>12</sup> CO	(+)-ephedrine	–3.6
<i>meso</i> -4- <sup>13</sup> CO	(+)-ephedrine	–7.1

separation of triplet radical pairs to form free radicals.<sup>19</sup> To develop a supramolecular approach for enantioselective reactions involving geminate radical pairs in zeolite supercages, two features of the pair must be controlled: (1) the separation of the geminate pair must be restrained so that geminate recombination has a high probability, and (2) the geminate recombination must be made enantiomerically selective. The first feature is achieved by generating a prochiral geminate pair in the supercage of a zeolite. The second feature is achieved by adding a chiral co-guest to the supercage.<sup>40</sup>

Imagine a zeolite supercage containing a ketone capable of producing a prochiral geminate pair that is adsorbed in a zeolite supercage together with a chiral co-guest and is designed so that a certain rotational motion and diffusional separation of the pair is possible, but that the size/shape features of the supramolecular structure encourage the pair to reencounter and to undergo geminate recombination. Each recombination of the geminate primary pair must produce either the (+) or the (–) enantiomer of the ketone, but in the presence of the chiral inductor, a certain enantiomeric selectivity may result. Analogous ideas have been applied to achieve striking enantiomeric selectivities in the reaction of *biradicals* adsorbed in zeolites.<sup>41</sup>

An example<sup>42</sup> of the successful application of the above strategy for enantiomeric selectivity in radical pair recombination has been achieved in the photolysis of d,l-**4** and *meso*-**4** in NaY zeolite in the presence of chiral inductors (Table 2). The photolysis of either d,l-**4** or *meso*-**4** in FAU zeolites was shown to have a significant probability of recombination of the primary geminate pair.<sup>34</sup> The probability of geminate recombination is probably limited by the rate of decarbonylation of primary geminate pairs. Enantiomeric selectivity<sup>42</sup> for the recombination of the primary radical pairs formed from photolysis of *meso*-**4** was achieved employing either (+)- or (–)-ephedrine as chiral inductors (Figure 8). Representative results are given in Table 2 for the photolysis of *meso*-**4** in NaY. The ee (enantiomeric excess) generated by (–)-ephedrine as a chiral inductor is equal and opposite to that generated by (+)-ephedrine as a chiral inductor.

### Magnetic Isotope Effects on the Enantiomeric Selectivity of Geminate Radical Pair Recombination

If the recombination of the primary triplet geminate pair is limited by the rate of intersystem crossing to the singlet pair, then the enantiomeric selectivity may be subject to magnetic isotope effects as was the case for the regioselectivity of primary pairs formed from photolysis of



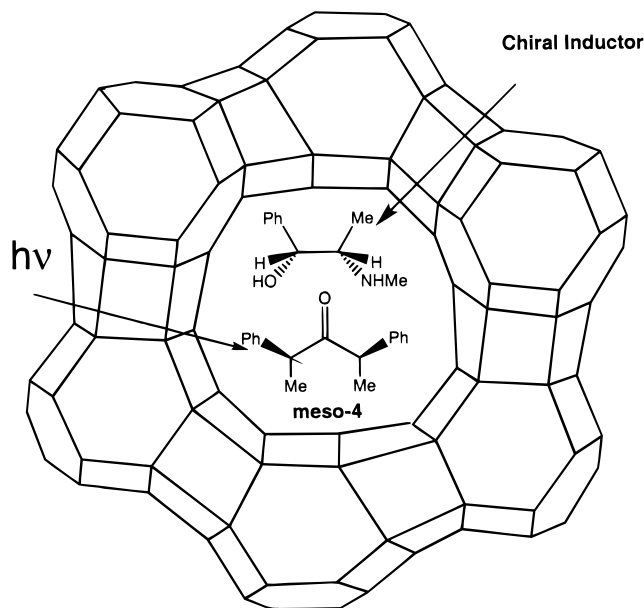


FIGURE 8. Schematic of the supramolecular structure of *meso-4*@NaY containing a chiral co-guest (ephedrine) in the supercage.

**1**@NaX. Effective diastereomeric interactions between the geminate pair and the chiral inductor will occur on a certain time scale; thus, the enantiomeric selectivity can be influenced by the *lifetime* of the triplet radical pair. This would be the case if the geminate pair–inductor interaction is too long or too short for optimal supramolecular enantiomeric interactions with the chiral inductor. If the lifetime of triplet geminate pairs in supramolecular systems is determined by ISC and if the rate of ISC can be controlled by magnetic isotope effects, the exciting possibility exists that *magnetic isotope effects can be employed to control the enantiomeric selectivity of geminate pairs in zeolites.*

Table 2 shows a remarkable  $^{13}\text{C}$  isotope effect on the ee of the d,l-**4** produced in the photolysis of *meso-4*@NaY with co-guest ephedrine as a chiral inductor. The ee increases by ca. 100% upon going from *meso-4*- $^{12}\text{C}$ O to *meso-4*- $^{13}\text{C}$ O! The remarkable difference in ee between *meso-4*- $^{12}\text{C}$ O to *meso-4*- $^{13}\text{C}$ O is ascribed to a  $^{13}\text{C}$  magnetic isotope effect on the rate of ISC in the primary geminate radical pair, exactly analogous to the  $^{13}\text{C}$  magnetic isotope found in the formation of the regioisomers of **1**. The magnetic moment of the  $^{13}\text{C}$  nucleus hyperfine couples to the unpaired electron on the  $^{13}\text{C}$ O radical of the primary geminate radical pair and increases the rate of ISC. This faster rate of ISC results in a higher probability and faster rate of recombination than the  $^{12}\text{C}$  radical pair (which undergoes ISC more slowly) under the influence of the chiral inductor. The possibility is supported by the observation that the *meso-4*- $^{12}\text{C}$  undergoes more decarbonylation than *meso-4*- $^{13}\text{C}$ , consistent with a longer lifetime of the radical pair produced from *meso-4*- $^{12}\text{C}$ .

## Summary

The chemistry of radicals@MFI and radicals@FAU is remarkable in that the products of radical–radical reac-

tions can be controlled by supramolecular effects and magnetic isotope effects. For DBKs adsorbed on MFI zeolites, supramolecular features of the initial ketone@MFI can be manipulated so that the secondary radicals can be made to undergo strong positive cage effects (secondary geminate recombination on the internal surface), strong negative cage reaction (sieving followed by size/shape controlled combination on the external and internal surface), or zero cage effects (random coupling on the external surface). In the case of photolysis of **4**@MFI, the preferred radical–radical reaction is disproportionation at the intersections, whereas radical–radical combination is the preferred reaction in solution. Radicals that can be adsorbed into the internal surface are persistent to an extent determined by supramolecular steric effects for radical–radical reaction at the intersections.

In the case of DBKs (**1**–**6**) adsorbed on FAU zeolites, the supramolecular features can be manipulated to achieve radical–radical reactions of the primary geminate radical pair. The regioselectivity of primary pair recombination may be controlled by supramolecular steric effects imposed by cations and co-guest molecules in the supercages. Enantiomeric selectivity in the recombination of the primary geminate pair may be achieved by including a chiral molecule as a co-guest in the supercage. Magnetic isotope effects on both regioselectivity and enantioselectivity have been observed.

Zeolites possess two apparently contradictory attributes: they are solids, yet they possess considerable void space. Such a contradiction was addressed over 2000 years ago by Lucretius<sup>43</sup> in his view of the nature of the solid state:

...Things are not hemmed in by the presence of solid bodies in a tight mass. This is because there is a vacuity in things. By vacuity I mean intangible and empty space. If such empty space did not exist, things could not move at all. Nothing could proceed, because nothing would give it a starting point by receding. — Lucretius, *On the Nature of the Universe*, ca. 200 B.C.

*The generous support of the National Science Foundation through Grant CHE 98-12676 and of the National Science Foundation and Department of Energy through Grant CHE 98-10367 to the Environmental Molecular Science Institute (EMSI) at Columbia is gratefully acknowledged. The author thanks all present and former students, postdocs, and visiting scientists who worked in his laboratory at Columbia over the years and whose contributions helped to make this review possible, especially Bruce Baretz, Peter Wan, Chen-Chin Cheng, Xue-gong Lei, Zhenyu Zhang, Miguel Garcia-Garibay, Naresh Ghatlia, Nikolas Kaprinidis, Margaret Landis, Wei Li, Sean Liu, Steffen Jockusch, M. Francesca Ottaviani, Zhiqiang Liu, and George Lem. He also thanks colleagues from industry for collaborations: Edith Flanigen (Union Carbide), Lloyd Abrams (DuPont), David Corbin (DuPont), and Paul Krusic (Dupont). Professor Ann McDermott (Columbia University) is thanked for providing insights to the use of solid state magnetic resonance spectroscopy. Special thanks go to Professor V. Ramamurthy (Tulane) for long-standing fruitful collaborations on all aspects of things photochemical.*

## References

- (1) Breck, D. W. *Zeolite Molecular Sieves*; R. E. Krieger: Malabar, FL, 1984.
- (2) Derouane, E. G. New Aspects of Molecular Shape-Selectivity: Catalysis by Zeolite ZSM-5. In *Catalysis by Zeolites*; Imelik, B., Ed.; Elsevier: Amsterdam, 1980; pp 5–18.
- (3) (a) Venuto, P. B. Organic Catalysis Over Zeolites: A Perspective on Reaction Paths within Micropores. *Microporous Mater.* **1994**, *2*, 297–411. (b) Derouane, E. G. Molecular Shape-Selective Catalysis by Zeolites. In *Zeolite: Science and Technology*; Ribeiro, F. R., Ed.; Martinus, Nijhoff Publ.: The Hague, 1984; pp 347–370.
- (4) *Catalysis Looks to the Future*; National Academy Press: Washington, DC, 1992; p 19.
- (5) Cronstedt, A. F. Observation and Description of an Unknown Species of Rock, Called Zeolites. *K. Vetensk. Acas. Handl.* **1756**, *77*, 120–130.
- (6) Ramamurthy, V.; Eaton, D. F.; Caspar, J. V. Photochemical and Photophysical Studies of Organic Molecules Included within Zeolites. *Acc. Chem. Res.* **1992**, *25*, 299–307.
- (7) Scaiano, J. C.; Garcia, H. Intrazeolite Photochemistry: Toward Supramolecular Control of Molecular Photochemistry. *Acc. Chem. Res.* **1999**, *32*, 783–793.
- (8) Turro, N. J.; Garcia-Garibay, M. A. Thinking Topologically About Photochemistry in Restricted Spaces. In *Photochemistry in Organized and Constrained Media*; Ramamurthy, V., Ed.; VCH: New York, 1991; pp 1–38.
- (9) Ramamurthy, V. Photochemistry of Organic Molecules Included in Zeolites. In *Photochemistry in Organized and Constrained Media*; Ramamurthy, V., Ed.; VCH: New York, 1991; pp 429–493.
- (10) Flanigen, E. M.; Bennett, J. M.; Grose, R. W.; Cohen, J. P.; Patton, R. L.; Kirchner, R. M. Silicalite, A New Hydrophobic Crystalline Silica Molecular Sieve. *Nature* **1978**, *271*, 512–516.
- (11) Olson, D. H.; Kokotailo, G. T.; Lawton, S. L.; Meier, W. M. Crystal Structure and Structure Related Properties of ZSM-5. *J. Phys. Chem.* **1981**, *85*, 2238–2443.
- (12) Herron, N. Toward Si-Based Life: Zeolites As Enzyme Mimics. *Chemtech* **1989**, 542–548.
- (13) Parton, R.; De Vos, D.; Jacobs, P. A. Enzyme Mimicking with Zeolites. In *Zeolite Microporous Solids: Synthesis, Structure and Reactivity*; Derouane, E. G., Lemos, F., Naccache, E., Ribeiro, F. R., Eds.; Kluwer Academic Publishers: Dordrecht, 1992; pp 555–578.
- (14) (a) Weiss, R. G.; Ramamurthy, V.; Hammond, G. S. Photochemistry in Organized and Confining Media: A Model. *Acc. Chem. Res.* **1993**, *26*, 530–536. (b) Ramamurthy, V.; Weiss, R. G.; Hammond, G. S. A Model for the Influence of Organized Media on Photochemical Reactions. *Adv. Photochem.* **1993**, *18*, 69–234.
- (15) Turro, N. J. *Modern Molecular Photochemistry*; University Science Books: Sausalito, CA, 1991; Chapter 13.
- (16) Fischer, H. Unusual Selectivities of Radical Reactions by Internal Suppression of Fast Modes. *J. Am. Chem. Soc.* **1986**, *108*, 3925–3927.
- (17) Griller, D.; Ingold, K. U. Persistent Carbon Centered Radicals. *Acc. Chem. Res.* **1976**, *9*, 13–19.
- (18) Turro, N. J.; Cheng, C.-C.; Abrams, L.; Corbin, D. R. Size, Shape and Site Selectivities in the Photochemical Reactions of Molecules Adsorbed on Pentasil Zeolites. *J. Am. Chem. Soc.* **1987**, *109*, 2449–2456.
- (19) (a) Step, E. N.; Buchachenko, A. L.; Turro, N. J. The Cage Effect in the Photolysis of (S)-(+)- $\alpha$ -Methyldeoxybenzoin: Can Triplet Radical Pairs Undergo Geminate Recombination in Non-Viscous Homogeneous Solution? *J. Org. Chem.* **1992**, *57*, 7018–7026. (b) Porter, N. A.; Krebs, P. J. Stereochemical Aspects of Radical Pair Reactions. In *Topics in Stereochemistry*; Eliel, E. L., Milen, S. H., Eds.; Wiley-Interscience: New York, 1988 pp 97–127.
- (20) Lunazzi, L.; Ingold, K. U.; Scaiano, J. C. Absolute Rate Constants for the Decarbonylation of the Phenylacetyl Radical. *J. Phys. Chem.* **1983**, *87*, 529–530.
- (21) Turro, N. J.; Gould, I. R.; Baretz, B. H. Absolute Rate Constants for Decarbonylation of Phenylacetyl and Related Radicals. *J. Phys. Chem.* **1983**, *87*, 531–532.
- (22) Turro, N. J.; Lei, X.; Li, W.; McDermott, A.; Abrams, L.; Ottaviani, M. F.; Beard, H. S. Photochemistry and Magnetic Resonance Spectroscopy as Probes of Supramolecular Structures and Migration Pathways of Organic Molecules and Radicals Adsorbed on Zeolites. *Chem. Commun.* **1998**, 695–696.
- (23) Turro, N. J.; McDermott, A.; Lei, X.; Li, W.; Abrams, L.; Ottaviani, M. F.; Beard, H. S.; Houk, K. N.; Beno, B. R.; and Lee, P. S. Photochemistry of Ketones Adsorbed on Size/Shape Selective Zeolites. A Supramolecular Approach to Persistent Carbon Centered Radicals. *Chem. Commun.* **1998**, 697–698.
- (24) Gomberg, M. An Instance of Triphenylmethyl. *J. Am. Chem. Soc.* **1900**, *22*, 757–771.
- (25) Reteý, J. Enzyme Reaction Selectivity by Negative Catalysis or How Do Enzymes Deal with Highly Reactive Intermediates? *Angew. Chem., Int. Ed. Engl.* **1990**, *29*, 355–361.
- (26) Hirano, T.; Li, W.; Abrams, L.; Krusic, P. J.; Ottaviani, M. F.; Turro, N. J. Reversible Oxygenation of a Diphenylmethyl Radical Rendered Supramolecularly Persistent. *J. Am. Chem. Soc.* **1999**, *121*, 7170–7171.
- (27) Hirano, T.; Li, W.; Abrams, L.; Krusic, P. J.; Ottaviani, M. F.; Turro, N. J. Supramolecular Steric Effects as the Means of Making Reactive Carbon Radicals Persistent; Quantitative Characterization of the External Surface of MFI Zeolites through a Persistent Radical Probe and a Langmuir Adsorption Isotherm. *J. Org. Chem.* **2000**, *65*, 1319–1330.
- (28) Jockusch, S.; Hirano, T.; Liu, Z.; Turro, N. J. A Spectroscopic Study of Diphenylmethyl Radicals and Diphenylmethyl Carbon Cations Stabilized by Zeolites. *J. Phys. Chem. B* **2000**, *104*, 1212–1216.
- (29) For examples of laser flash photolysis investigations of diphenylmethyl adsorbed on zeolites, see: Kelly, G.; Willsher, C. J.; Wilkinson, F.; Netto-Ferreira, J. C.; Olea, A.; Weir, D.; Johnston, L. J.; Scaiano, J. C. Diffuse Reflectance Laser Flash Photolysis and Product Studies of Diphenylmethyl Radicals on Solid Supports. *Can. J. Chem.* **1990**, *68*, 812–819.
- (30) A similar reversible oxygenation was found for triphenylmethyl in a matrix: Janzen, E. G.; Johnson, F. J.; Ayers, C. L. The Reversible Thermal Decomposition of Triphenylmethylperoxy Radical to Triphenylmethyl Radical and Oxygen. *J. Am. Chem. Soc.* **1967**, *89*, 1176–1183.
- (31) Turro, N. J. Photochemistry of Organic Molecules in Microscopic Reactors. *Pure Appl. Chem.* **1986**, *58*, 1219–1228.
- (32) Turro, N. J.; Zhang, Z. Photochemistry of Molecules Adsorbed on Alkali Ion Exchanged Zeolites. A ‘Lebensraum’ Effect on Product Formation. *Tetrahedron Lett.* **1987**, *28*, 5637–5640.
- (33) Turro, N. J.; Wan, P. Photolysis of Dibenzyl Ketones Adsorbed on Zeolite Molecular Sieves. Correlation of Observed Cage Effects with Carbonyl  $^{13}\text{C}$  Enrichment Efficiencies. *J. Am. Chem. Soc.* **1985**, *107*, 678–682.
- (34) Ghatlia, N. D.; Turro, N. J. Diastereoselective Induction in Radical Coupling Reactions: Photolysis of 2,4-Diphenylpentan-3-ones Adsorbed on Faujasite Zeolites. *J. Photochem. Photobiol. A: Chem.* **1991**, *57*, 7–19.
- (35) Ramamurthy, V.; Turro, N. J. Photochemistry of Organic Molecules within Zeolites: Role of Cations. *J. Inclusion Phenom. Mol. Recognit. Chem.* **1995**, *21*, 239–282.
- (36) Zhang, Z. Photochemistry of Dibenzyl Ketone and Its Derivatives Adsorbed on Size/Shape Selective Zeolites. Ph.D. Thesis, Columbia University, 1989.
- (37) Turro, N. J.; Buchachenko, A. L.; Tarasov, V. F. How Spin Stereochemistry Severely Complicates the Formation of a Carbon–Carbon Bond between Two Reactive Radicals in a Supercage. *Acc. Chem. Res.* **1995**, *28*, 69–78.
- (38) Turro, N. J.; Kraeutler, B. Magnetic Field and Magnetic Isotope Effects in Organic Photochemical Reactions. *Acc. Chem. Res.* **1980**, *13*, 369–377.
- (39) Turro, N. J.; Zhang, Z. Magnetic Isotope and Magnetic Field Effects on the Product Distributions of Photolyses of Dibenzyl Ketone Adsorbed on Zeolites. *Tetrahedron Lett.* **1989**, *30*, 3761–3764.
- (40) Kaprinidis, N.; Landis, M. S.; Turro, N. J. Supramolecular Control of Photochemical Enantiomeric Induction and Radical Pair Recombination in Zeolites. *Tetrahedron Lett.* **1997**, *38*, 2609–2702.
- (41) Sundarababu, G.; Leibovitch, M.; Corbin, D. R.; Scheffer, J. R.; Ramamurthy, V. Zeolite as a Host for Chiral Induction. *Chem. Commun.* **1996**, 2159–2160.
- (42) Lem, G.; Turro, N. J. Radical Pair Recombination Stereoselectivity as a Probe of Magnetic Isotope and Magnetic Field Effects. *Chem. Commun.* **2000**, 293–294.
- (43) Lucretius, *On the Nature of the Universe*; Translated by Latham, R. E.; Penguin Books: New York, 1951; p 37.

AR980103A